

Inoue, T., et al., 2023, Waterfall height sets the mechanism and rate of upstream retreat: *Geology*, <https://doi.org/10.1130/G51039.1>

Supplemental Material

Table S1. Summary of experiment results

Figure S1.

Supplemental Information

Additional Experimental Methods

Previous experiments have simulated bedrock using concrete mixtures (Yamaguchi et al. 2017; Mishra et al. 2018; Inoue and Nelson, 2020), cohesive materials (Grimaud et al., 2016), and polyurethane foam (Scheingross et al., 2017, Scheingross and Lamb, 2019). In this study, we use a homogeneous concrete mixture of 1-part White Portland cement to 50-parts 0.34 mm diameter silica sand to 8-parts water by weight. Based on previous experiments (Yamaguchi et al. 2017), we set the concrete mixture hard enough to resist erosion from clear water flow, but weak enough to allow erosion via the particle impacts. At the beginning of all three experiments (prior to turning on the sediment feed and initiating erosion), the water depth both upstream of the waterfall (measured sufficiently far above the waterfall lip to avoid the drawdown influence (Haviv et al., 2006)) and downstream of the waterfall was ~ 0.8 cm and the flow velocity was ~ 0.49 m/s. This resulted in fully turbulent (Reynolds number of ~ 4000) and supercritical (Froude number of ~ 1.7) flow, thus providing dynamic similarity of flow conditions relative to other incising bedrock rivers (Lamb et al., 2015).

We roughly scaled the morphology of our experiments to match the waterfall at Oiran-buchi (Fig. 1). The channel slope (2%) and waterfall face angle (45°) approximately match those of Oiran-buchi. In Run 1, we set the waterfall drop height to $\sim 1/100$ th of the waterfall drop height in Oiran-buchi. The flow depth and flow discharge in Run 1 were chosen to achieve a ratio of drop height to flow depth of 6.0, which roughly matches observations of maximum drop height to flow depth for Oiran-buchi and South Fork Silver Creek (4.4 and 7.5, respectively, see the next section below). We increased the waterfall drop height in Run 3 to create a drop height to flow depth ratio of 25 while holding the flow depth for Run 3 at the same value as in Run 1. The drop height to flow depth ratio of 25 is an approximate average of the maximum values at Unokonotaki and Niagara Falls (18.5 and 30.5, respectively, see the next section below). In this way, Runs 1 and 3 were designed as end-member cases to approximately match field examples of waterfalls retreating via cyclic step erosion (Run 1) and headwall undercutting (Run 3). We set the drop height in Run 2 to be approximately midway between Run 1 and Run 3.

We set the sediment grain size to 1.4 mm, resulting in a critical Shields stress of ~ 0.07 at the beginning of each experiment in the section upstream of the waterfall. We chose this sediment size as a balance between the need for all sediment to be fully mobile at the start of the experiment while maximizing the particle Reynolds number (Re_p) (Lamb et al., 2015). The 1.4 mm sediment results in particle Reynolds numbers of ~ 60 , large enough for the critical Shields stress for sediment motion to be independent of Re_p (Buffington and Montgomery, 1997). Coincidentally, the 1.4 mm size is roughly $1/100$ th of the sediment in the area around Oiran-buchi, matching the $1/100$ scaling we used to set the waterfall drop height in Run 1. We set the channel width to 5 cm ($1/8000$ th of Oiran-buchi) for ease of experimental logistics, and adjusted the sediment supply rate to be $\sim 30\%$ of the expected load required for the initial concrete bed to become fully

alluviated. This ensured that there was ample sediment available as tools to erode the bed, while minimizing the effect of sediment cover.

We measured topographic change at the end of each experiment by first removing all deposited sediment with a vacuum cleaner and then pouring plaster over the eroded portion of the channel. This allowed us to make a mold of the terrain (Fig. S1d, e). We destroyed the eroded concrete to expose the plaster, and then used a 3D scanner (Artec EVA) to make a point cloud of the plaster mold at an approximate resolution of 1 point per 0.5 mm. We measured the waterfall retreat distance from the mold as the distance from the lip of the initial waterfall to the lip of the uppermost waterfall (which we defined as the furthest upstream step that had a drop height equal to or larger than the initial waterfall) at the conclusion of the experiment. We also measured the averaged angle of upstream migrating waterfall face from multiple traces of vertical drilling carved into the mold (see Fig. 2 side view).

Point cloud data from our experiments are available via the following repository: <https://zenodo.org/record/7869714#.ZEN-J3bP0Q8>.

Estimating waterfall drop height to flow depth ratios for field examples

We estimated the ratio of waterfall drop height to flow depth for Unokonotaki, Niagara Falls, Oiran-buchi, and South Fork Silver Creek (Fig. 1) using a combination of published data, field measurements, and theory. For Unokonotaki (32.6925673, 131.1845719), we measured a 24 m waterfall drop using a DEM published by the Geospatial Information Authority of Japan. Estimating a bankfull flow depth above the waterfall was slightly more complicated. In a town ~1.5 km upstream of the falls, a flood warning is issued at flow depths of 1.3 to 1.8 m, and we use this value as an estimate of the bankfull depth.

For Niagara Falls (43.0772635, -79.07467580), we make estimates at Horseshoe Falls using the Philbrick (1970) profile, which shows a drop height of ~61 m (accounting for both the ~56 m drop from the waterfall lip to water surface of the Maid of Mist Pool and the ~5 m depth between the water surface and the Grimsby Sandstone bedrock lip that serves as the downstream end of the Horseshoe Falls plunge pool). The normal flow depth in the upper Niagara River upstream of Niagara Falls varies from ~2 to 7 m depth (National Oceanic and Atmospheric Administration Chart 14832), resulting in a drop height to flow depth ratio of ~8.7 – 30.5.

For Oiran-buchi (42.9872018, 141.3369729), we estimate a 5 m drop height (Yamaguchi et al., 2017) and a flow depth of ~1.1 to 2.7 m based on Manning's uniform depth ($h = (Q_w n / w \sqrt{s})^{3/5}$), where Q_w is the volumetric water discharge, w is channel width, s is bed slope, h is flow depth, and n is Manning's roughness coefficient which we estimate following Garcia (2008) as $n = D_{84}^{1/6} / (8.1g^{1/2})$. Full grain size distribution for the bed at Oiran-buchi are not available, but surveys from the Hokkaido Development Bureau in 1978, 1995 and 2006 give average grain sizes (D_{50}) ranging from 58 mm to 530 mm and we use these measurements to calculate a range of Manning's n (n

$= D_{50}^{1/6} / (8.1g^{1/2})$) from $0.025 < n < 0.035$. Forty-five years of flow data collected by the Ishiyama flow station (~3 km upstream of the study site) show an average annual peak flow of ~283 m³/s, with the highest recorded flood of 834 m³/s. The average width and slope of the 400 upstream reaches of this site are 40 m and 0.02, respectively.

Finally, we estimated the drop height to flow depth for the series of small cyclic steps in South Fork Silver Creek (Fig. 1f) during a field survey of 11 waterfalls at low flow conditions. Waterfall drop height at this location ranged from 0.3 m to 4.5 m, with an average height of 1.8 m. We estimate bankfull flow depth for South Fork Silver Creek using the same method as done for Oiran-buchi above. For South Fork Silver Creek, average channel width and slope are 10 m and 8.4%, respectively. We estimate Manning's $n = D_{84}^{1/6} / (8.1g^{1/2})$ following (Garcia, 2008) and we set $D_{84} = 0.36$ m based on a random walk pebble count conducted upstream of the cyclic steps. Five years of flow data collected by the California Department of Water Resources (~1 km downstream of the study site) show an average annual peak flow of ~8 m³/s, which yields a flow depth of 0.24 m using the Manning's Equation above, with the largest recorded flood of 38.2 m³/s yielding a flow depth of 0.61 m. Based on our average waterfall drop height of 1.8 m, we estimate the drop height to flow depth ratio ranges from 3.0 to 7.5.

Theory predictions of cyclic step wavelength

Theory for bedrock cyclic step formation (Izumi et al., 2017) use both the Froude number at the threshold of bedrock erosion (threshold Froude number), Fr_t , and the corresponding bed slope at the threshold of bedrock erosion (threshold slope), S_t , as input parameters. The threshold Froude number and slope are defined as the case when, in a steady, uniform (normal) threshold state for incision, the bedrock is just barely drowned in alluvium. Calculating Fr_t and S_t requires an estimate of critical Shields number for sediment motion on a bedrock bed, which is ~0.017 in this experiment from the method of Inoue et al., (2014). Although Shields number is not determined by the Froude number alone, under the conditions of this experiment, a flow with Froude number of 0.6 will have a Shields number of 0.017.

In Run 1, the Froude number in the uniform state observed in the upstream reach of the initial step was $Fr_n = 1.7$, and the bed slope was 0.02. Following Izumi et al. (2017), Fr_t for these conditions must be between 0.53 and 0.9 in order for cyclic steps to form (see Fig. 8 in Izumi et al. (2017)). For the following calculations we set $Fr_t = 0.6$, and also show the results of using $Fr_t = 0.53$ and $Fr_t = 0.9$ at the end of this section. In the steady, uniform threshold state, and the steady, uniform state observed in Run 1, we have the relations

$$C_f Fr_t^2 = S_t \quad (S1)$$

$$C_f Fr_n^2 = S \quad (S2)$$

where C_f is the bed friction coefficient. If the bed friction coefficient C_f is assumed to be constant, combining Eqs. (S1) and (S2) reduce to

$$S_t = \left(\frac{Fr_t}{Fr_n} \right)^2 S \quad (S3)$$

Substituting $Fr_t = 0.6$, $Fr_n = 1.7$, and $S = 0.02$ into Eq. (S3), yields $S_t = 0.0025$.

The Froude numbers Fr_t and Fr_n are defined, respectively, by

$$Fr_t^2 = \frac{u_{td}^2}{gh_{td}}, \quad Fr_n^2 = \frac{u_{nd}^2}{gh_{nd}} \quad (S4, S5)$$

where u_{td} and h_{td} are the velocity and the flow depth in the uniform threshold state respectively, u_{nd} and h_{nd} are the velocity and the flow depth in the uniform state observed in Run 1 respectively, and g is the gravitational acceleration. Denoting the flow discharge per unit width by q_{wd} , conservation of mass requires that

$$q_{wd} = u_{td}h_{td} = u_{nd}h_{nd} \quad (S6)$$

Equations (S3) - (S6) reduce to

$$h_{td} = \left(\frac{S}{S_t} \right)^{1/3} h_{nd} \quad (S7)$$

Substituting $S = 0.02$, $S_t = 0.0025$, and $h_{nd} = 0.8$ cm into Eq. (S7), yields $h_{td} = 1.6$ cm.

We can compare this result to theoretical predictions shown in Fig. 9c of Izumi et al. (2017), which shows the dimensionless wavelength L as functions of Fr_n . Under these conditions, when $Fr_n = 1.7$, $L = 0.021$. Because the dimensionless wavelength L is normalized by h_{td}/S_t , the dimensional wavelength L_d is written in the form

$$L_d = \frac{h_{td}}{S_t} L \quad (S8)$$

Substituting $h_{td} = 1.6$ cm, $S_t = 0.0025$, and $L = 0.021$ into Eq. (S8), yields $L_d = 0.13$ m. Repeating this series of calculations with $Fr_t = 0.53$ and $Fr_t = 0.9$ bounds the

dimensional wavelength between $4.6 \text{ cm} < L_d < 18.8 \text{ cm}$; these values bound our Run 1 experimental observations of an $\sim 13 \text{ cm}$ wavelength between cyclic steps

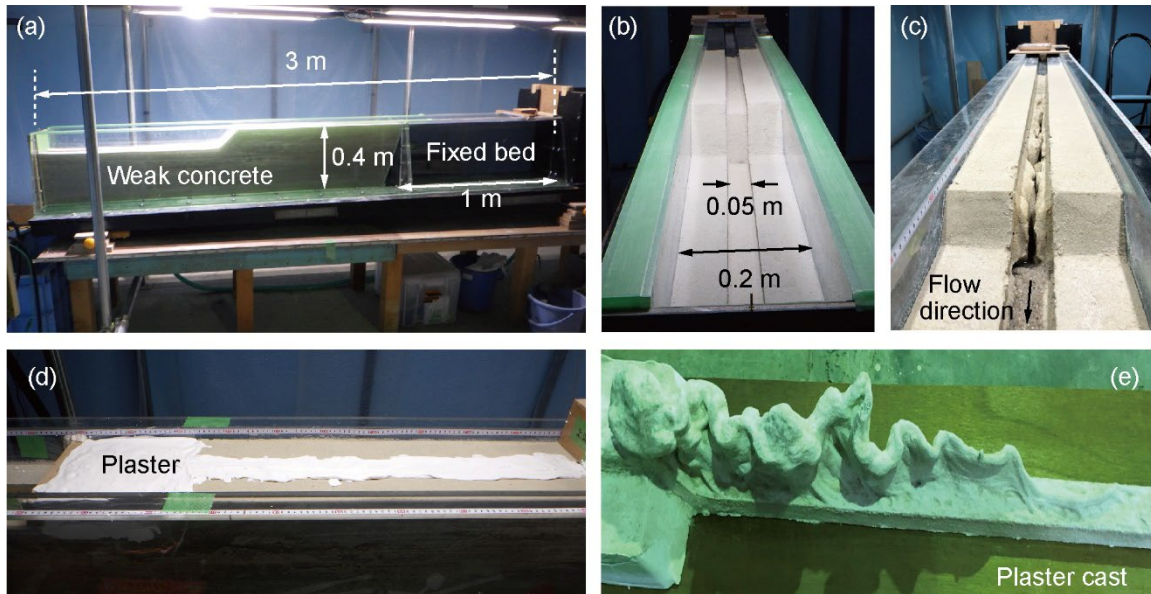


Figure S1. Overview of the experiment, (a) side-view of experimental channel, (b) initial experimental channel seen from downstream, (c) a narrow-eroded channel after the end of Run 1, (d) plaster poured into the eroded channel, (e) the plaster cast of Run 1 removed after solidification.

References for Supplementary Information

- Buffington, J. M., and Montgomery, D. R., 1997, A systematic analysis of eight decades of incipient motion studies, with special reference to gravel-bedded rivers: *Water Resources Research*, v. 33(8), p. 1993–2029, doi: 10.1029/96WR03190.
- Garcia, M.H., 2008, Sediment transport and morphodynamics. *in* Garcia, M. H. ed., *Sedimentation Engineering: Processes, Measurements, Modeling, and Practice*: American Society of Civil Engineers, Reston, VA, p. 21–163, doi: 10.1061/9780784408148.
- Grimaud, J.L., Paola, C., and Voller, V., 2016, Experimental migration of knickpoints: influence of style of base-level fall and bed lithology: *Earth Surface Dynamics*, v. 4, p. 11–23, doi: 10.5194/esurf-4-11-2016.
- Haviv, I., Enzel, Y., Whipple, K.X., Zilberman, E., Stone, J., Matmon, A., and Fifield, L. K., 2006, Amplified erosion above waterfalls and oversteepened bedrock

reaches: *Journal of Geophysical Research*, v. 111, F04004, doi: 10.1029/2006JF000461.

- Inoue, T., and Nelson, J.M., 2020, An experimental study of longitudinal incisional grooves in a mixed bedrock–alluvial channel: *Water Resources Research*, v. 56, e2019WR025410, doi: 10.1029/2019WR025410.
- Inoue, T., Izumi, N., Shimizu, Y., and Parker, G., 2014, Interaction among alluvial cover, bed roughness, and incision rate in purely bedrock and alluvial-bedrock channel: *Journal of Geophysical Research: Earth Surface*, v. 119, p. 2123–2146, doi: 10.1002/2014JF003133.
- Izumi, N., Yokokawa, M., and Parker, G., 2017, Incisional cyclic steps of permanent form in mixed bedrock-alluvial rivers: *Journal of Geophysical Research: Earth Surface*, v. 122, p.130–152, doi: 10.1002/2016JF003847.
- Lamb, M. P., Finnegan, N. J., Scheingross, J. S. and Sklar, L. S., 2015, New Insights into the Mechanics of Fluvial Bedrock Erosion through Flume Experiments and Theory: *Geomorphology*, v. 317, p. 233, doi: 10.1016/j.geomorph.2015.03.003.
- Mishra, J., Inoue, T., Shimizu, Y., Sumner, T., and Nelson J. M., 2018, Consequences of abrading bed load on vertical and lateral bedrock erosion in a curved experimental channel: *Journal of Geophysical Research: Earth Surface*, v. 123, p. 3147– 3161, doi: 10.1029/2017JF004387.
- Philbrick, S.S., 1970, Horizontal Configuration and the Rate of Erosion of Niagara Falls: *Geological Society of America Bulletin*, v. 81(12), p. 3723–3732, doi: 10.1130/0016-7606(1970)81[3723:HCATRO]2.0.CO;2.
- Scheingross, J.S., Lamb, M.P., and Fuller, B.M., 2019, Self-formed bedrock waterfalls: *Nature*, v. 567, p. 229– 233, doi: 10.1038/s41586-019-0991-z.
- Scheingross, J.S., Lo, D.Y., and Lamb, M.P., 2017, Self-formed waterfall plunge pools in homogeneous rock: *Geophysical Research Letters*, v. 44, p. 200–208, doi: 10.1002/2016GL071730.
- Yamaguchi, S., Inoue, T., Maeda, I., Sato, D., Shimizu, Y., 2017, Knickpoint survey in Toyohira River and experiment of collision of gravel particles to the knickpoint: *Journal of JSCE (Hydraulic Engineering)*, v. 73(4), p. I_913– I_918, doi: 10.2208/jscejhe.73.I_913.